Robotica (2010) volume 28, pp. 311–319. © Cambridge University Press 2009
doi:10.1017/S0263574709990385

Modeling of blade sharpness and compression cut of biomaterials

Debao Zhou†* and Gary McMurray‡

†*Department of Mechanical and Industrial Engineering, University of Minnesota, Duluth, MN 55812, USA*
‡*Food Processing Technology Division, ATAS Laboratory, Georgia Tech Research Institute, Atlanta, GA 30332, USA*

(Received in Final Form: July 23, 2009. First published online: September 21, 2009)

SUMMARY

To realize the automation of biomaterial cutting, the interaction between the blade and biomaterial deserves insight understanding. In this paper, a blade-compression cutting model is developed. The influences from the material properties, deformation, and blade properties on the cutting force are thoroughly explained. An approach to describe the sharpness of a blade is provided and its applicability is experimentally demonstrated. Based on the material property and knife sharpness property, the required force to realize compression cut can be predicted. This provides the reference force trajectory for the automation of biomaterial compression cutting.

KEYWORDS: Modeling; Blade; Compression cut; Sharpness.

1. Introduction

Recently, applications of robotics have been extended from traditional industry (i.e., automobile) to more broad field relating to human's everyday life, such as the medical operation and food processing. Along with such progress on robotics application, the tasks required from robots have become much more complicated. The goal of this research is to develop automated machines to perform cutting operations on parts with unknown size. The initial task for our development is the chicken wing-shoulder cutting operation in a poultry-processing factory. It is the task that directly affects the yield of the breast meat, which is the highest profit margin item on a bird. High volume of such cutting everyday is an onerous job for human operators. Since the tasks involve processing animal carcasses, there are safety considerations in addition to being very labor intensive. There is a high risk of musculoskeletal disorders (MSDs) which are often attributed to the forces, postures, and repetition of the meat-processing tasks.[1] Thus, robotics implementation on the cutting operation is desired.

In order to accomplish this, a thorough understanding of the science behind cutting is necessary. Food cutting is different from metal cutting in which food is highly deformable while metal is not. During cutting, the formation of the offcuts plays a major role in the amount of energy required to cause cutting. Metal cutting creates plastically deformed offcuts, which permanently store energy while the elastically deformed food offcuts, in materials such as cheese, fruit, etc, permanently store almost no energy. Thus many researchers have formulated the food cutting problems using energy method. Mahvash and Hayward[2] formulated the relationship between the cutting force and blade moving distance during deformation, cutting, and rupture through application of the fracture toughness concept.[3] Atkins *et al.*[4] have been able to explain why there is smaller force requirement when pressing and slicing compared to pressing only. Atkins and Mai[5] provided the value of the fracture toughness for some biomaterials. Starting from energy aspects, Kamyab *et al.*[6] formulated the stress and force distribution in cheese cutting.

The internal stress method has also been used to explain what is going on during cutting. Yoshihara and Matsumoto[7] studied the shearing properties of wood using the stress analysis method. They mainly considered the average shear stress. Through the in-plane shear test using a thin specimen, they obtained some of the material properties, such as the shear modulus and shear strength.

In addition to the properties of the materials to be cut, blade sharpness is another important factor that affects the required cutting forces. The contact between the cutting object and the blade is a small area, which can be shown from the microstructure of a knife. Tech Edge[8] has documented the microstructure of their knife products. Bishu *et al.*[9] performed a laboratory study of forces used in cutting a bologna with a sharp knife and a dull knife. In the medical industry, Black *et al.*[10] discussed the influence of scalpel blade sharpness on the pain level and healing conditions. Brown *et al.*[11] experimentally measured the cutting force in food processing based on different blade sharpness. In order to reduce the occurrence of fracture and overturning when topping with blunted knives and to reduce the loss of working time in replacing blunted knives, Moore *et al.*[12] experimentally investigated the influence of knife edge geometry. Some of the works have been summarized by Reilly *et al.*[13] Kamyab *et al.*[6] studied the force per unit length of a wire cheese cutter with various wire diameters and cutting speeds. Blade sharpness also directly influences the cutting moments and the grip forces applied by an operator. McGorry *et al.*[14] studied the magnitude of the grip force and moment using three kinds of blades with different sharpness, i.e., polished knives, smooth knives, and coarse knives. They found that a finely polished knife significantly reduced mean grip force and cutting moment. Szabo *et al.*[15] developed a procedure to establish knife steeling schedules

* Corresponding author. E-mail: dzhou@domn.edu

https://doi.org/10.1017/S0263574709990385 Published online by Cambridge University Press

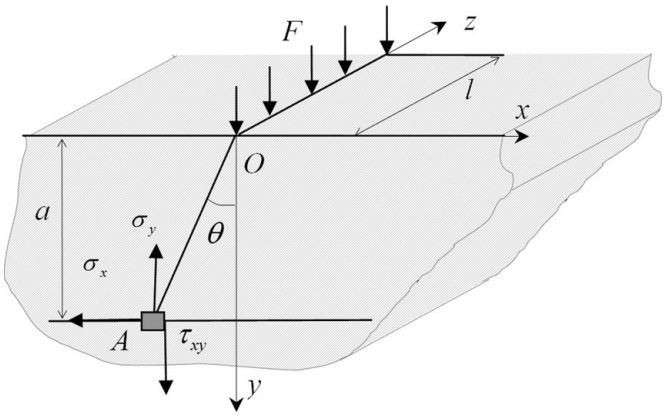


Fig. 1. Simplified model for prefracture cuts.

based on increased force resulted from knife dullness after repeat usages, in order to minimize operator exertions and physical stress associated with work-related musculoskeletal disorders. Szabo *et al.*[15] used the edge area formed when a blade cuts into a material made by carrageenan, a kind of transparent gel at room temperature, to quantify the blade sharpness. McCarthy *et al.*[16] presented a numerical and experimental investigation into the forces generated when cutting biomaterials with surgical scalpel blades. An elastomer with similar nonlinear mechanical properties to human skin was chosen as a reference material for the investigation. They also derived a quantitative index of blade sharpness via indentation experiments in which elastomeric materials were cut using both sharp and blunt straight edge blade.[17]

The above research results provided important explanations about the cutting of biomaterials. However, the fundamental cutting principles still remain unclear such as what stress generates this fracture and how a blade influences the cutting. In order to provide more practical and insight understanding, this research uses internal stress to describe the cutting mechanism and the sharpness of a set of blades. In the following, based on a simplified compression cutting model, the stress distribution in the cutting materials and the fracture criterion are described. A relative sharpness factor is then defined to describe the relationship between the applied force and the knife dullness. Finally, numerical results and experimental results are used to verify the formulation. By providing the explanation of the compression cutting mechanism, the force during compression cutting can be predicted and knife sharpness can be monitored.

2. Modeling and Explanation

The simplified model for prefracture compression cut of food products using straight-edge blade is shown in Fig. 1, where the blade edge is along the z-axis of the frame $Oxyz$ and the y-axis is the cutting direction. In this analysis, several assumptions have been made:

(i) The cutting motion of the blade is assumed to be a translation along the $+y$ direction.
(ii) Cutting was constrained to be compression.
(iii) The applied force on the knife edge is uniform in the normal direction of the contact plane.
(iv) The moving speed of the knife along y-axis direction is slow such that it is valid to be considered as static cutting.
(v) The friction between the sides of the blade and the object is neglected. This assumption can be evaluated in two cases. The first case is that the object is in tension, such as the cutting of chicken shoulder joint. In this case, there will be no contact between the side of the blade and the adjacent cut material immediately after cutting, i.e., the cut part will move away from the knife due to the pulling force of the chicken wing in the magnitude of several Newton. The second case is that the object is not in tension. In such case, the friction force can be obtained when the blade moves out of the material after cutting. Then the actual cutting force is obtained from the subtraction of the withdrawn force from the total force.

2.1. Modeling of blade compression cutting

In the blade-compression cutting system, the cutting force can be modeled as either a concentrated or distributed force F acting on a semi-infinite plane as shown in Fig. 1. In Fig. 1, σ_x, σ_y, and τ_{xy} are the stresses at point A, whose location is decided by parameters (a, θ, P). The physical meaning of P is the load per unit contact area, which is defined later in Eq. (4). According to Timoshenko,[18] the stresses at point A can be expressed as

$$\sigma_y = -\frac{2P}{\pi a}\cos^4\theta, \tag{1a}$$

$$\sigma_x = -\frac{2P}{\pi a}\cos^2\theta\sin^2\theta, \tag{1b}$$

$$\tau_{xy} = -\frac{2P}{\pi a}\sin\theta\cos^3\theta. \tag{1c}$$

Based on the definitions of the fracture criteria by Michael,[19] failure can occur as a result of any of the following cases shown in Eqs. 2(a–c),

$$\left|-\frac{2P}{\pi a}\cos^4\theta\right| \geq \frac{\sigma_{uy}}{K_s}, \tag{2a}$$

$$\left|-\frac{2P}{\pi a}\cos^2\theta\sin^2\theta\right| \geq \frac{\sigma_{ux}}{K_s}, \tag{2b}$$

$$\left|\frac{2P}{\pi a}\sin\theta\cos^3\theta\right| \geq \frac{\tau_{uxy}}{K_s}, \tag{2c}$$

where σ_{ux}, σ_{uy}, τ_{uxy}, and K_s are the ultimate tensile strength, ultimate compression strength, ultimate shear strength[20] and cutting fracture concentration factor, respectively.

During the compression cutting process there are two sets of failure criterions for the material, i.e., prior to fracture and postfracture. Prior to material fracture, all of the stress in the material is due to deformation therefore the cutting fracture concentration factor, $K_s = 1$. Once the stress within the material reaches one of the failure criterions given in Eq. (2), the material will fracture and cause crack formation

https://doi.org/10.1017/S0263574709990385 Published online by Cambridge University Press

at the point of failure. After the fracture is initiated, the initial failure criterion ($K_s = 1$) is no longer valid due to the cutting fracture concentration occurring at the tip of the crack. During postfracture, the cutting fracture concentration factor needs be determined using

$$K_s = F_{\text{fracture}} \big/ F_{\text{cutting}}, \tag{3}$$

where F_{fracture} is the applied forces at the initiation of the fracture and F_{cutting} is the force at postfracture (during the continuous cut). Since the applied forces at the initiation of the fracture (F_{fracture}) and postfracture (F_{cutting}) can be measured during actual cutting, the value of K_s can then be determined experimentally using Eq. (3).

2.2. *External force, pressure, and deformation*

We consider the ith small portion of the knife edge with length Δl, width w_i with cutting force ΔF. Then the pressure at that small area is

$$P = \frac{\Delta F}{w_i \Delta l}, \tag{4}$$

Normally, the width of a blade edge may vary along z-axis, or,

$$\Delta F = P w_i \Delta l. \tag{5}$$

As an example, the relationship between the external force and the compression stress satisfies,

$$\Delta F = -\frac{\sigma_y \pi a}{2\cos^4\theta} w_i \Delta l. \tag{6}$$

The stress–strain relationship can be expressed as $\sigma_y = E\varepsilon_y$, where E is the Young's modulus of the material. Note that in case of elastic deformation, E is a constant, for other cases, E changes with different deformation (for biomaterials). Thus

$$\Delta F = -E\left(\frac{\pi a}{2\cos^4\theta}\right)(w_i \Delta l)\varepsilon_y, \tag{7}$$

where Δl is contact length and$\pi a/2\cos^4\theta$ is related to the location (θ) of the interested point. With fixed material property, cutting contact length, and point location, the deformation ε_y is proportional to the applied external force, locally. In the location where the stress is maximum

$$\Delta F = -E\left(\frac{\pi a_{\max}}{2\cos^4\theta_{\max}}\right)(w_i \Delta l)\,\varepsilon_{y\max}, \tag{8}$$

where $\varepsilon_{y\max}$ expresses the maximum strain when external force ΔF is applied to the material on Δl and $\theta_{\max}$ and $a_{\max}$ express the location where the maximum stress occurs. By defining

$$K_{\max} = -E\pi a_{\max} \big/ 2\cos^4\theta_{\max},$$

there is

$$\Delta F = K_{\max} w_i \Delta l \varepsilon_{y\max}. \tag{9}$$

For a razor blade, the force is generated along a straight line, and a_{max} and θ_{max} do not change in the z direction. Thus there is

$$F = \int \mathrm{d}F = \sum \Delta F = K_{\max}\varepsilon_{y\max} \times \sum w_i \Delta l = K_{\max}\varepsilon_{y\max} \int w_i \mathrm{d}l.$$

By defining the average width of the knife edge as

$$w = \lim_{n\to\infty} \frac{\sum_{i=0}^{n} w_i}{n},$$

there is

$$F = K_{\max}\varepsilon_{y\max} l w, \tag{10}$$

where l is the effective cutting length, and F the total force acting on the object. Since K_{max} relates to material property E and maximum stress location (θ), Eq. (10) shows that for certain material, at the maximum deformation location, the cutting force is linearly depends on the contact length and the average blade width when a razor blade is used.

2.3. *Equivalent fracture force*

Immediately following fracture, one of the Eqs. 2(a–c) holds. Suppose the fracture is due to compression, there is

$$\left| -\frac{1}{w_i}\frac{2\cos^4\theta_u}{\pi a_u}\frac{\Delta F_u}{\Delta l} \right| = K_{uy} \tag{11}$$

where K_{uy} is a material-dependent constant and ΔF_u is the applied external force on length Δl when fracture occurs, θ_u and a_u are the location of the point where fracture happens. When a razor blade is used, the cutting force is generated along a straight line. Along the z-axis, a_u and θ_u do not change. By setting

$$K_u = \left| -\frac{\pi a_u K_{uy}}{2\cos^4\theta_u} \right|, \tag{12}$$

there is

$$\Delta F_u = K_u w_i \Delta l = \xi_u \Delta l, \tag{13}$$

where ξ_u is both material- and knife-dependent parameter. Integrating both side of Eq. (13) in the case of the straight edge (e.g., razor blade compression cut), there is

$$F_u = \xi_u l. \tag{14}$$

Based on Eq. (14), by analyzing the experimental results between l and F_u, we can calculate ξ_u for a specific material and a razor blade. Thus, for an actual application where ξ_u is known, the cutting force can be predicted for a given length of cut.

https://doi.org/10.1017/S0263574709990385 Published online by Cambridge University Press

2.4. Relative blade sharpness factor

During the actual cutting application, it is normally impossible to measure the width at every point of the edge. Alternatively, we define a relative value, the blade relative sharpness factor η, to replace the average width of the knife edge. It is defined as

$$\eta = \frac{w}{w_0},$$

where w_0 is the average edge width of the sharpest blade (brand new blade) in the applied bladed set. Then, immediately following fracture, the cutting force and the blade relative sharpness factor can be expressed as

$$F_u = K_u w l = K_\eta \eta w_0, \tag{15}$$

where $K_\eta = K_u l$ is a constant when the contact length does not change. In the sharpest case, such as a brand new blade from manufacturer, there is

$$\eta_0 = F_{u0}/(K_\eta w_0). \tag{16}$$

The knife relative sharpness can be expressed as

$$\eta = \eta_0 F_u / F_{u0}. \tag{17}$$

In the dullest case, the maximum allowable force has to be applied in order to realize cutting, then there is

$$\eta_f = \eta_0 F_{uf} / F_{u0}. \tag{18}$$

For simplification, we define another parameter, knife relative sharpness level, κ as

$$\kappa = \text{int}\left(\frac{(n-1)(\eta - \eta_0)}{\eta_f - \eta_0} + 1\right), \tag{19}$$

where n is a user-defined integer used to distinguish the sharpness level of a blade and int(#) rounds the element # to the nearest integer. Thus a knife can be categorized into n-level sharpness starting from level 1 by defining $\eta_0 = 1$ for the sharpest blade as defined in Eq. (16).

3. Numerical Verification

In this part, a static cutting process is modeled by ANSYS software to verify the formulation of the stress distribution in Section 2. The properties of the selected material (raw potato) at the static case are $E = 100$ Pa and Poisson's ratio $\nu = 0.45$.[21] The material is shaped as a large rectangular plate to simulate a half semi-infinite plane (the x–y plane as shown in Fig. 1). A concentrated force is added to the middle of the upper boundary. The lower boundary is fixed in space. This model is with the same boundary constraints and loading method for the potato and chicken meat in the cutting experiments in Section 4 as shown in Fig. 3, i.e., only the bottom surface of the material is fixed and all the other surfaces are free.

When the applied concentrated force is 0.4536 Kg, the generated deformation and stresses are shown in Fig. 2. From the shear stress distribution, it can be seen that the maximum shear stress (0.0371 Pa) occurs immediately next to the point of the application with the concentrated force (Fig. 2 a, b). The maximum compression stress (0.2730 Pa) is at the point just beneath the external force (Fig. 2 d). The maximum tensile stress (0.1179 Pa) occurs at the point with the application in the direction of the applied force (Fig. 2 c).

It is also observed that the maximum forces are related as: $\sigma_y = 7.76\tau_{xy}$ and $\sigma_y = 2.32\sigma_x$. The compression stress and the tension stress are significantly larger than the shear stress. Thus, if the ultimate shear, compression, and tensile strengths are known for a material, the stress caused the cutting fracture can be distinguished.

Further numerical results indicate that the maximum stress is proportional to the magnitude of the external force, and the location of the maximum strength is always in the same position relative to the acting point, which proves that the K_{max} and K_u are constant in Eqs. (10) and (13).

4. Experimental Results and Discussion

For the experimental demonstration of the models in Section 2, a baking potato and chicken breast are selected as the cutting objects. This potato is taken as a reference material due to the fact that its material properties as well as its fracture toughness are known[5] and the documented properties are used to validate the experimental results.

The experimental setup is shown in Fig. 3. The system consists of an ABB robot IRB 140[22] for motion generation, speed control and distance measurement, and an ATI Force/Torque sensor[23] for force measurement. The robot is commanded to move at a very low speed (0.5 mm/s) for cutting. The data of the force are saved on a central computer with sampling rate at 20 Hz.

4.1. Force, displacement, and equivalent fracture force

The first experiment was performed to determine the relationship between the applied force and the corresponding displacement (blade moving distance) as well as that between the fracture force and the contact length. The obtained cutting forces using potatoes are shown in Fig. 4, where the ordinate represents the compression force in Newton (N) and the abscissa is the blade moving distance in millimeter (mm). Note that in Fig. 4, the cutting results are obtained using the same blade with three contact lengths, 5 mm, 16 mm, 24 mm, respectively. The results obtained from chicken meat cut are shown in Fig. 5.

During both the chicken meat and potato cuts, the cutting force increases as the blade moves. When the compression force reaches a certain value, material fracture occurs. In the potato cut, this happens at 9.79 N with contact length 24 mm; while the force is 10.45 N in chicken meat cut with a contact length of 15 mm. After that, the cutting force drops to a lower value, i.e., 6.45 N in potato cut and 7.12 N in chicken meat cut, and then remains almost constant with only small variations due to fluctuations in material properties throughout the sample. The abrupt drop in cutting force is due to the release of strain energy once the blade has penetrated into the material. These results reflect similar cutting characteristics for both chicken meat and potato cuts.

https://doi.org/10.1017/S0263574709990385 Published online by Cambridge University Press

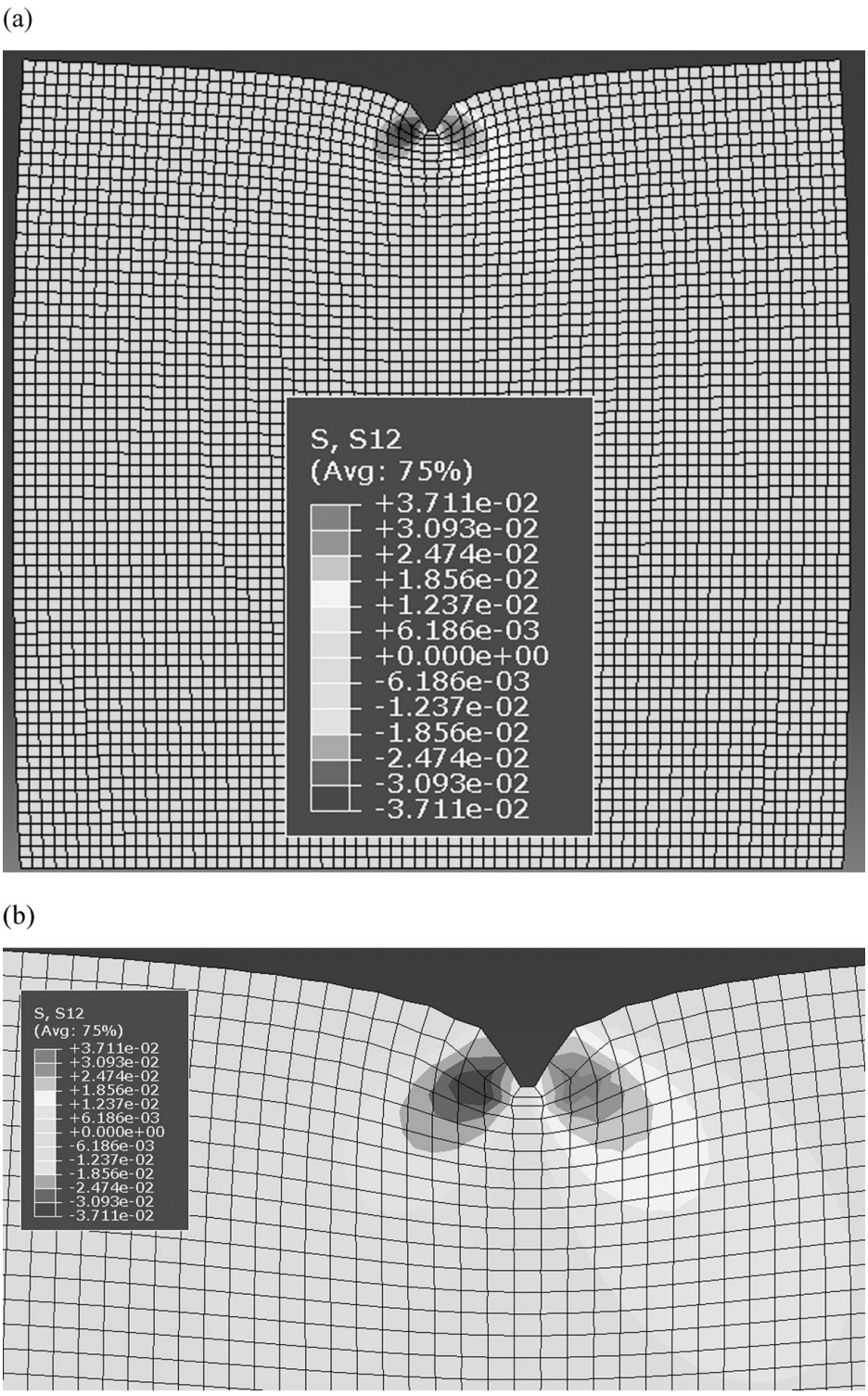


Fig. 2. For legend see next page.

Therefore a complete analysis using compression cutting from a potato is applicable to the chicken meat and other biological materials.

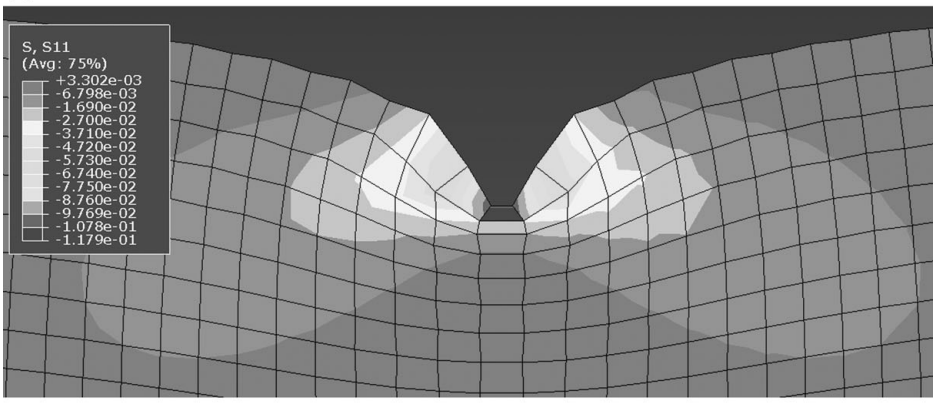
Based on the material deformation, i.e., relationship between the external force and the moving distance of the blade, Young's modulus for the chicken meat and the potato can be calculated using the Hertzian Method.[24]

The relationship between the fracture force and the contact length in a potato cut is shown in Fig. 6, where the abscissa is the contact length in mm and the ordinate is the fracture force in N. The fracture force and the contact length (l) are linearly related with linearity $R^2 = 0.9846$ and slope $\xi_u = -0.3874$. Note that the linear relationship is expressed in Eq. (14).

When prefracture cutting force is normalized by the contact length, it can be seen in Fig. 7 for the blade moving distance from 0 mm to 1.2 mm that the slopes of all the curves for the contact lengths 5 mm, 16 mm, and 24 mm are about −0.3803 N/mm. The constant slope, which is expressed by K_{max} in Eq. (10), represents the constant ratio between the force and deformation.

https://doi.org/10.1017/S0263574709990385 Published online by Cambridge University Press

(c)



(d)

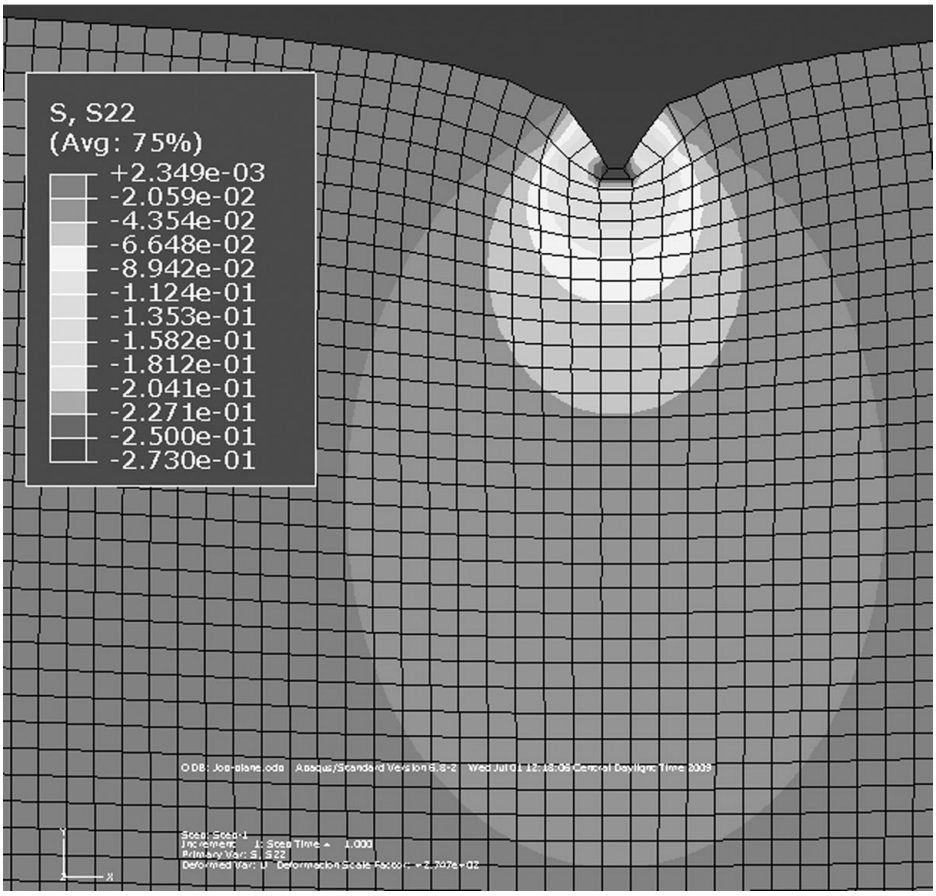


Fig. 2. Numerical results of the stress distribution of the semi-infinite half-plane with concentrated external force. (a) τ_{xy}; (b) detailed view of the shear stress distribution near the fore acting point; (c) detailed view of σ_x; (d) detailed view of σ_y.

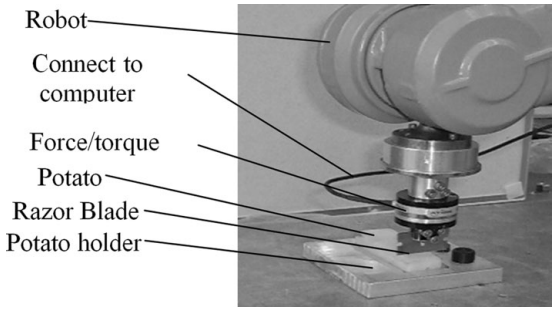


Fig. 3. Experimental setup.

Fig. 8 shows the change of the cutting force (postfracture force) with the contact length. During cutting, the cutting force looks like white noise as shown in Figs. 4, 5 and 7, which fluctuates with the small variation of material properties, around a constant value. The average cutting force is linearly related to the contact length with a slope of -0.2469.

Atkins and Mai[5] provided the fracture toughness of potato as 0.2 kJ/m^2. From our experiments, the relationship between the applied force and contact length is 0.2469 N/mm or 0.2469 kJ/m^2 which agrees well with Atkins and Mai's result. This validates the experiments.

https://doi.org/10.1017/S0263574709990385 Published online by Cambridge University Press

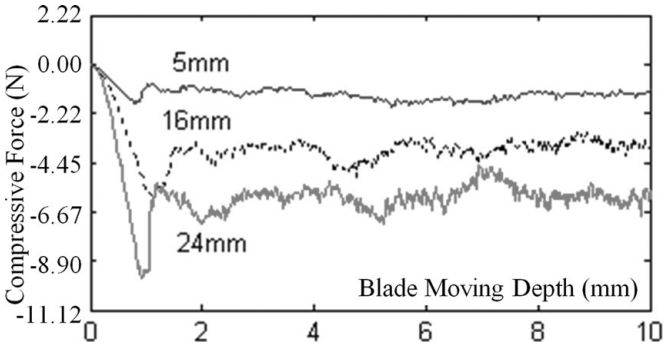


Fig. 4. Cutting force change with blade moving distance for potato cuts.

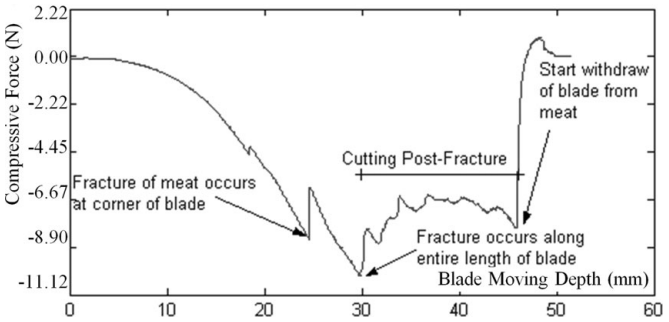


Fig. 5. Cutting force change with blade moving distance for chicken meat cut.

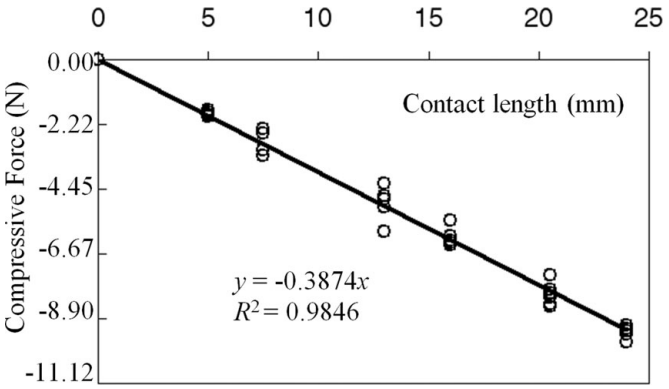


Fig. 6. Fracture force and contact length.

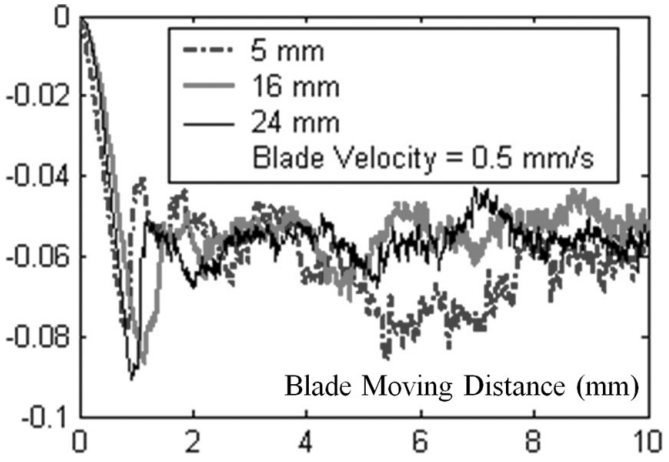


Fig. 7. Normalized cutting force with contact length.

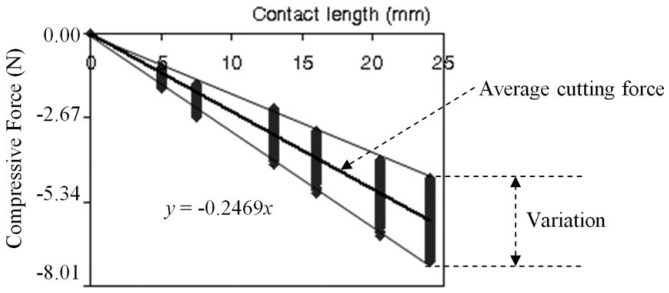


Fig. 8. Relationship of cutting forces and contact length.

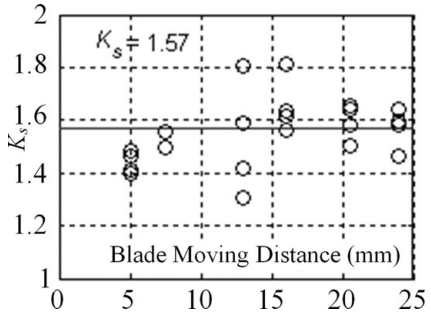


Fig. 9. Determination of K_s in potato cuts.

From the potato and chicken meat cutting results shown in Figs. 4 and 5, the ratio between the prefracture force and the postfracture force K_s can be calculated and the calculated results from potato are shown in Fig. 9. In Fig. 9, the K_s values are calculated for four cuts at the contact lengths of 5 mm, 13 mm, 16 mm, 20.5 mm, and 24 mm, respectively. In addition, we also show two cuts at the contact length of 7.5 mm. It is noticed that the K_s is almost constant for any contact length and the value is around 1.57.

4.2. Evaluating relative blade sharpness factor

This part of the experiments is used to demonstrate how to implement the sharpness method defined in this paper. In the experiments described in Section 4.1, we use the same knife with different lengths to distinguish the effect from the contact length. In this section, we use blades with different sharpness to cut the same material to study the effect of blade sharpness. The materials (potato) were prepared in rectangular shape with the same width and thickness (13 mm in width and 30 mm in thickness) to make sure the contact length of each cut was same. The blades are prepared such that sharpest blade and the dullest blade defined in Eqs. (16–18) are included. The procedure of the blade preparation is as follows: (1) choose a brand-new blade (industrial-grade single-edge razor blade standard, 0.2286 mm thick) as the sharpest one, blade A, define its relative sharpness $\eta_0 = 1$ and obtain the cutting forces using this blade (Blade A); (2) use the sharpest blade (Blade A) to manually cut cardboard 30 times to form blade B and obtain the cutting forces using this blade; (3) use Blade B to cut through a piece of pine wood 50 times to form blade C and obtain the cutting forces using this blade; (4) Blade C is dulled on aluminum by rubbing 30 times to form blade D and obtain the cutting forces using this blade; (5) the dullest knife is obtained by dulling Blade D on sand paper (aluminum oxide cloth sanding sheet 80 grit)

https://doi.org/10.1017/S0263574709990385 Published online by Cambridge University Press

Table I. Blade relative sharpness level.

Blade #	Force at fracture (N)				Average force (N)	η (relative sharpness factor)	κ *(relative* sharpness level)
A	5.20	6.49	6.36	6.67	6.18	1	1
B	7.87	7.16	7.92	7.78	7.70	1.24	2
C	10.23	9.65	10.19	10.76	10.19	1.65	3
D	12.01	11.17	12.14	11.57	11.74	1.89	4
E	15.79	15.75	16.28	15.35	15.79	2.55	5

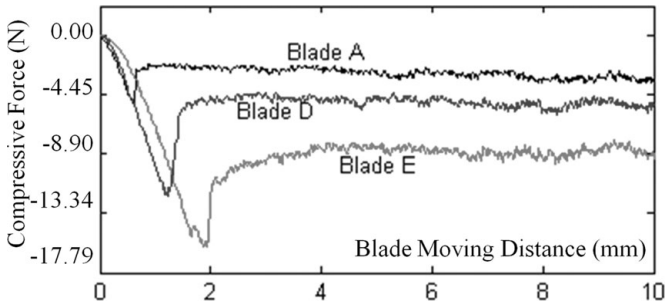


Fig. 10. Cutting results using different sharpness blades (only Blade A, D, E are shown).

by 10 times, obtain the cutting forces using this blade; (6) according to the cutting forces of the sharpest blade (Blade A) and the dullest blade (Blade E) to get η_f; (7) set sharpness level (n) of Blade E is 5 ($n = 5$) and according to Eq. (19) to specify the sharpness level κ to which another blade belongs. Part of the obtained force results are shown in Fig. 10 and the blade sharpness level results are summarized in Table I. In Table I, the first 4 columns show the fracture forces obtained from Fig. 10. Column 5 is the average fracture force. Relative blade sharpness level η and relative blade sharpness level κ are calculated based on Eqs. (17) and (19). From the last column in Table I, it can be seen that blades B, C, D are in the 2nd, 3nd, and 4th sharpness level, respectively.

By using this method, any blade can be assigned to a certain sharpness level. When the cutting force reaches certain level by which the knife is decided to be dull, the knife needs to be sharpened.

5. Conclusions

In this paper, the mechanics of biomaterial compression cutting in static state is studied. The relationships among the required pre- and postfracture force, blade property, and material properties are mathematically discussed and experimentally tested.

From both the mathematical model and experimental results, it is observed that the interaction of the blade and the material during cutting, i.e., the deformation and the cutting force, does not only depend on the material properties, but also linearly depend on the blade relative sharpness and the contact length. The force used to initial cutting fracture (fracture force) is greater than that during cutting fracture in the case of all the other parameters are the same, such as contact length and blade relative sharpness factor. Thus fracture force is used to specify the sharpness of a blade. By using the obtained cutting force data, the relative blade sharpness can be determined and its implementation is experimentally demonstrated.

To make the work more complete, in the future, the compression cutting mechanics will be extended to the analysis of the cutting due to slicing forces and further to the consideration of the dynamic factors such as relaxation and creep. This work establishes the theoretical foundation for the development of a control system to guide a robot to cut natural products with unknown geometries.

References

1. P. Dempsey and R. McGorry, "Investigation of a pork shoulder deboning operation," *J. Occup. Environ. Hygiene* **1**, 167–172 (2004).
2. M. Mahvash and V. Hayward, "Haptic rendering of cutting: A fracture mechanics approach," *Haptics-e* **2**(3), 1–12 (2001).
3. K. Hellan, *Introduction to Fracture Mechanics* (McGraw-Hill, New York, 1984).
4. A. Atkins, X. Xu and G. Jeronimidis, "Cutting, by 'pressing and slicing,' of thin floppy slices of materials illustrated by experiments on cheddar cheese and salami," *J. Mater. Sci.* **39**, 2761–2766 (2004).
5. A. Atkins and Y. Mai, *Elastic and Plastic Fracture: Metals, Polymers, Ceramics, Composites, Biological Materials* (Ellis Horwood, Chichester, UK, 1985).
6. I. Kamyab, S. Chalranarti and J. Williams, "Cutting cheese with wire", *J. Mater. Sci.* **33**, 2763–2770 (1998).
7. H. Yoshihara and A. Matsumoto, "Measurement of the shearing properties of wood by in-plane shear test using a thin specimen," *J. Int. Acad. Wood Sci.* **39**(2), 114–152 (2005).
8. Tech Edge Inc., http://www.furitechnics.com.au/information/Tech%20Edge/Cutting%20edge%20angles.htm, (2005).
9. R. R. Bishu, C. Calkins, X. Lei and A. Chin, "Effect of knife type and sharpness on cutting forces," *Adv. Occup. Ergon. Saf.* **2**, 479–483 (1996).
10. D. Black, R. Marks and A. Caunt, "Measurement of scalpel blade sharpness and its relationship to wound healing," *Bioeng. Skin* **1**, 111–123 (1985).
11. T. Brown, S. James and G. Purnell, "Cutting forces in food: Experimental measurements," *J. Food Eng.* **70**(2), 165–170 (2005).
12. M. A. Moore, F. S. King, P. F. Davis and T. C. D. Manby, "The effect of knife geometry on cutting force and fracture in sugar beet topping," *J. Agric. Eng. Res.* **24**(1), 11–27 (1979).
13. G. A. Reilly, B. A. O. McCormacka and D. Taylorb, "Cutting sharpness measurement: A critical review," *J. Mater. Process. Technol.* **153–154**, 261–267 (2004).
14. R. McGorry, P. Dowd and P. Dempsey, "The effect of blade finish and blade edge angle on forces used in meat cutting operations," *Appl. Ergon.* **35**, 71–77 (2005).
15. R. Szabo, R. Radwin and C. Henderson, "The influence of knife dullness on poultry processing operator exertions and

https://doi.org/10.1017/S0263574709990385 Published online by Cambridge University Press

the effectiveness of periodic knife steeling," *Am. Ind. Hygiene Assoc. J.* **62**(4), 428–433 (2001).
16. C. T. McCarthy, R. O'Dwyer, M. Hussey, M. D. Gilchrist and N. P. O'Dowd, "A Numerical and Experimental Investigation into the Forces Generated when Cutting Biomaterials," *Proceedings of the ASM International Conference on Materials and Processes for Medical Devices*, St. Paul, MN, (Aug. 25–27, 2004) pp. 140–145.
17. C. T. McCarthy, M. Hussey and M. D. Gilchrist, "On the sharpness of straight edge blades in cutting soft solids: Part I – Indentation experiments," *Eng. Fract. Mech.* **74**, 2205–2224 (2007).
18. S. Timoshenko, *Theory of Elasticity*, (Mcgraw-Hill book Company, New York, 1970).
19. W. Michael, *Stress Analysis of Fiber-Reinforced Composite Materials* (WCB McGraw-Hill, Boston, MA, 1998).
20. A. Recum and J. Jacobi, Handbook of Biomaterials Evaluation: Scientific, Technical and Clinical Testing of Implant Materials, Chapter 35, pp. 539–540.
21. M. Bourne, *Food Texture and Viscosity: Concept and Measurement* (Academic Press, New York, 2002).
22. ABB Inc., "Product Manual IRB 140, ABB Robotics Products AB publication," Article number: 3HAC 7564-1 (2000).
23. ATI Inc., "Installation and Operations Manual for ISA F/T-16," ATI Industry Automation Inc. publication, Manual PN 9610-05-1012-04 (1998).
24. A. Fischer-Cripps, "Introduction to contact mechanics," *Chapter 6* (Springer, New York, 2000) pp. 107.

https://doi.org/10.1017/S0263574709990385 Published online by Cambridge University Press